EQUIVALENT FRACTURE ENERGY CONCEPT FOR DYNAMIC RESPONSE ANALYSIS OF PROTOTYPE RC GIRDERS

Abdul Qadir Bhatti[1], Norimitsu Kishi[2] and Khaliq U Rehman Shad[3]

[1] *Assistant Professor, Dept. of Structural Engineering , School of Civil and Environmental Engineering, NUST, Pakistan & Postdoctoral Research Fellow Department of Civil Engineering, National University of Singapore*
[2] *Professor, Dept. of Civil Engineering and Architecture, Muroran Institute of Technology, Japan*
[3] *Leader Joint Working Group, Pakistan China University, Higher Education Commission Islamabad, Pakistan*
Email: cvebaq@nus.edu.sg & bhatti-nit@nust.edu.pk

ABSTRACT :

Here, in order to establish a modification method for material properties of concrete so as to rationally analyze the prototype RC girder with sand cushion using coarse mesh, an equivalent fracture energy concept for concrete elements was proposed and the applicability was investigated comparing numerical analysis results with experimental results. From this study, it is confirmed that even though coarse mesh was used for prototype RC girder with sand cushion, similar results with those obtained using fine mesh can be assured.

KEYWORDS: Sand cushion, prototype RC girder, Equivalent cracking energy, Drucker-Prager yield criterion, Impact resistant design, Impact response analysis

1. INTRODUCTION

Rock-sheds are used to protect lives and lifelines against these potential rock-impacts. Cushion materials are laid on the roof of rock-sheds to absorb the rock fall impact energy, which is one of the main input parameters in design of the rock-sheds and, still now these structures have been designed based on an allowable stress design concept using simply estimated maximum impact force [1]. However, in order to rationally design this type RC structures considering the performance up to ultimate state, impact resistant behavior and dynamic load-carrying capacity for those should be investigated precisely. For these, not only experimental study but also numerical analyses one should be performed.

The advantage of the proposed technique is that mesh size sensitivity on failure is removed leading to results, which converge to a unique solution, as the mesh is refined. The proposed algorithm has been validated by a full-scale prototype with sand cushion test results using different cases of mesh refinement. The algorithm has been implemented into LS-DYNA for hexahedron solid elements and correctly accounts for crack directionality effects with sand cushion [2]. Thus enabling the control of energy dissipation will be associated with each failure mode regardless of mesh refinement.

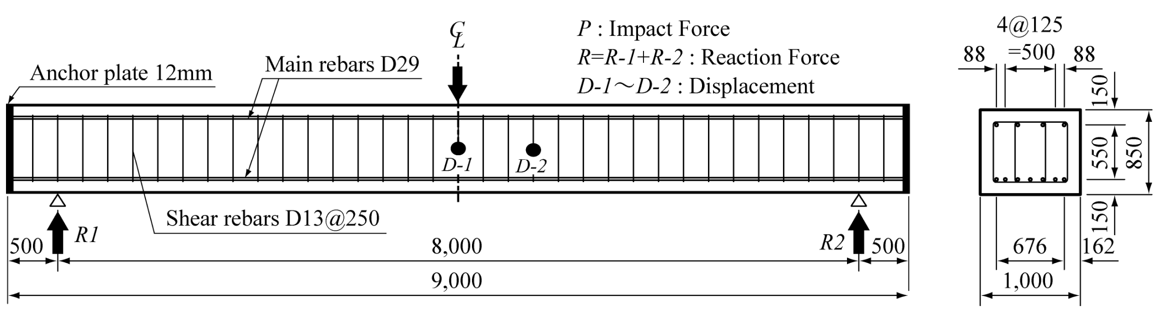

Figure 1 Dimensions of RC girder and measuring items

Table 2.1 Static design parameters of RC girder

Shear rebar ratio ρ_t	Static shear depth ratio a/d	Static shear capacity V_{usc} (kN)	Static bending capacity P_{usc} (kN)	Shear-bending capacity ratio α
0.0064	5.71	1794	619.8	2.894

Table 2.2 Material properties of concrete and rebar

Type	Density ρ ton/m^3	Elastic coefficient E GPa	Poisson's Ratio ν	Yielding strength MPa
Concrete	2.343	25.4	0.177	31.2
Rebar D13	7.85	206	0.3	390
Rebar D29				400

2. EXPERIMENTAL OVERVIEW

2.1 Dimensions and static design values

RC girder, which is modeled for roof of real RC rock-sheds, is taken for falling-weight impact test of prototype RC structures. The girder is of rectangular cross section and the dimensions are of 1 m x 0.850 m and clear span is 8 m long. The dimensions of the sand cushion set on the center of girder are of 1.5x1.5x0.9 m. Figure 1 shows dimensions of the RC girder, arrangement of rebars, and measuring points for each response wave. In this figure, it is confirmed that 7#D29 rebars are arranged which is for 0.64 % of main rebar ratio corresponding to designing of real RC rock-sheds and 4#D29 rebars are arranged as the upper axial rebar in which the rebar volume corresponds to half of main rebar ratio. Axial rebars were welded to 12 mm steel-plate at the height of 5 m ends for saving of anchoring length of the rebars. Thickness of concrete cover is assumed to be 150 mm as well as real rock-sheds. D13 stirrups are arranged with intervals of 250 mm which is less than a half of an effective height of the cross section. In this study, arranging interlayer stirrups and upgrading in shear load-carrying capacity, the RC girder with sand cushion was designed to be failed with flexural failure mode. The displacements of the girder were measured at mid-span (*D-1*) and the point (*D-2*) with the intervals of 750 mm from the mid-span. Impact force P was estimated using deceleration of the heavy weight, which was measured using accelerometers set at top surface of heavy weight. Reaction force R was also measured using load-cells installed in the supporting gigues. The detailed static design parameters of the RC girder are listed in Table 2.1. Static flexural and shear load-carrying capacities P_{usc} and V_{usc} were calculated based on standards specification of concrete structures in Japan [3]. From this table, it is confirmed that the RC girder designed here will fail with flexural failure mode under static loading. The static material properties of concrete and rebars during experiment are listed in Table 2.2.

2.2 Experimental Method

In the experiment, a 5,000 kg heavy weight was lifted up to the prescribed height of 5 m by using the track crane, and then dropped freely to the mid-span of girder with sand cushion due to a desorption device. A heavy weight is made from steel outer shell with 1 m in the diameter, 97 cm in height, and spherical bottom with 80 cm in radius and its mass is adjusted filling concrete and steel balls.

The RC girder was set on the supporting gigues, which are made so as to freely rotate but not to move toward each other. The ends of RC girder is fixed in the upward direction using steel rods and beams to prevent from jumping up at the time of impacted by a heavy weight. In this experiment, impact force wave (P), reaction force wave (R), and displacement waves (D) at two points along the girder were measured. Impact force wave was estimated using a deceleration of heavy weight, which is measured using accelerometers set at the top surface of the weight such as mentioned at previous paragraph. The accelerometer is of strain gauge type and its capacity and frequency range for measuring are 1,000 times gravity and DC through 7 kHz, respectively. Each

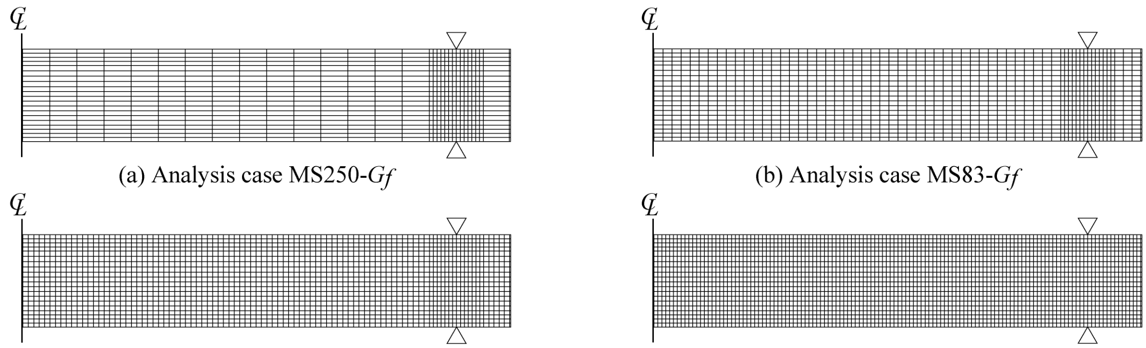

(a) Analysis case MS250-Gf (b) Analysis case MS83-Gf

(c) Analysis case MS50-Gf (d) Analysis case MS35-Gf

Figure 2 FE mesh size distribution for each analytical case

load-cell for measuring reaction force are of 1,500 kN capacity and more than 1 kHz measuring frequency. For measuring displacements, laser-type linear variable displacement transducers (LVDTs) were used which are of 200 mm maximum stroke and 915 Hz measuring frequency.

3. ANALYTICAL OVERVIEW

3.1 FE models

The purpose of this research is to propose the method for converting tensile strength of concrete element with arbitrary element size in span direction applying an equivalent fracture energy concept for full scale RC girder with sand cushion and the applicability was discussed by comparing with the experimental results. Therefore, the standard element division for precise numerical analysis result is needed. In this research, the suitable results were used and the standard analytical model such as MS35-G_f was decided for prototype RC girder with sand cushion. Similarly the standard mesh size of the span and the cross section width and height of direction of the RC girder with sand cushion were set as 35 mm, 41 mm and 31 mm, respectively, based on the previous results [4].

On the other hand, four cases were considered by assuming 1, 3, 5, and 7 divisions for the interval of 250 mm stirrup whose element sizes are 250 mm, 83 mm, 50 mm, and 35 mm, respectively, and those cases are named as MS250-G_f, MS83-G_f, MS50-G_f and MS35-G_f respectively. For all cases, each mesh size along the girder in the inside and outside area of 500 mm wide with respect to the supporting point was set to be 35 mm long because of precisely analyzing an interaction between supporting gigues and girders. The mesh size distribution of each analytical case is shown in Fig. 2.

One quarter of RC girder with sand cushion was three dimensionally modeled for numerical analysis with

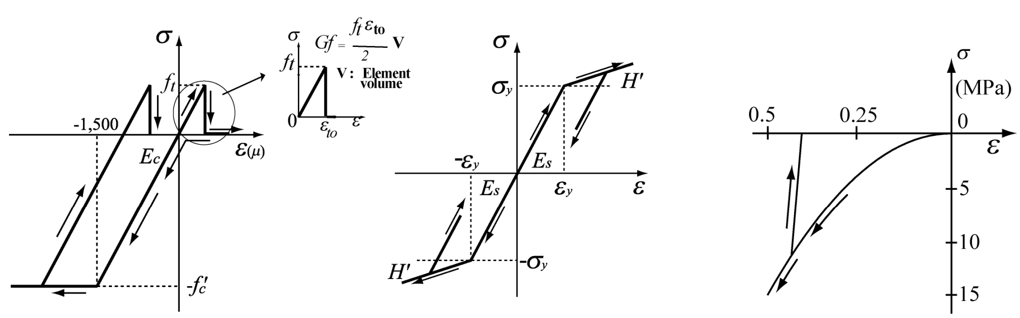

(a) Concrete Model (b) Rebar Model (c) Sand Model

Figure 3 Stress-strain relation of model

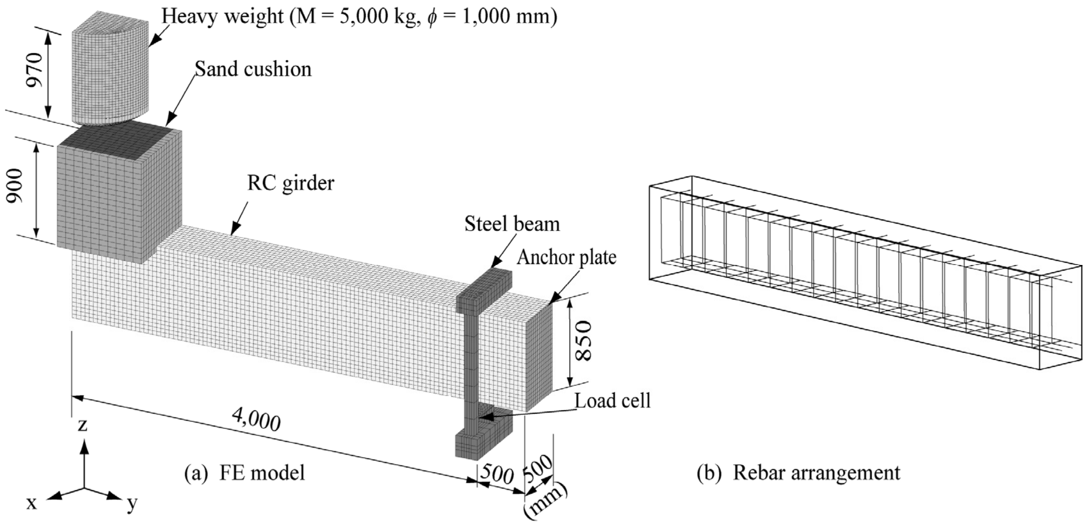

Figure 4 FE Numerical analysis model

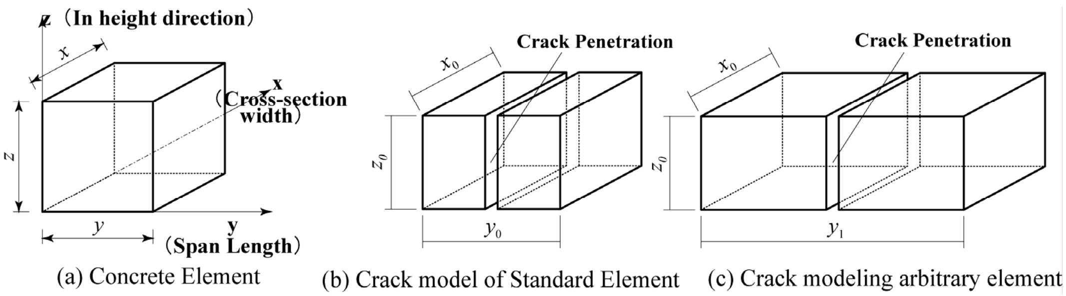

Figure 5 Crack modeling of an element

respect to the two symmetrical axis. Fig. 4 shows a mesh geometry of the girder with sand cushion, which is finally used for numerical analysis case of MS35-G_f. Geometrical configurations of the heavy weight and supporting gigue were also precisely modeled corresponding to the real ones. In this model, axial rebar and stirrup were modeled using beam element having equivalent axial stiffness, cross sectional area and mass with those of real ones. The others were modeled using eight-node and/or six-node solid elements.

Total number of nodal points and elements for one-fourth model for MS35-G_f, shown in Fig. 4 are 43,838 and 38,167, respectively. Number of integration points for solid and beam elements are one and four, respectively. In order to take into account of contact interface between concrete and head of heavy weight elements and between adjoining concrete and supporting gigue elements, contact surface elements for those were defined, in which contact force can be estimated by applying penalty methods for those elements but friction between two contact elements were neglected. Impact velocity of 9.8 m/sec for falling height of 5 m was applied to all nodal points of the falling heavy weight. Based on the previous experience viscous damping has been used for all cases of the numerical study [4].

3.2 Modeling of Materials

3..2.1 Concrete

Stress-strain relationships of concrete were assumed by using a bilinear model in compression side and a cut-off model in tension side as shown in Fig. 3(a). It is assumed that 1) yield stress is equal to compressive stress *f'c*; 2) concrete yields at 0.0015 strains; 3) tensile stress is perfectly released when an applied pressure reaches tensile strength of concrete; 4) tensile strength is set to be 1/10th of the compressive strength; and 5) von

Mises criterion was applied to the yielding of concrete [4].

3.2.2 Rebar

For main rebars and stirrups, an elasto-plastic model following isotropic hardening rule was applied as shown in Fig. 3(b). Here, the plastic hardening modulus *H'* was assumed to be 1% of elastic modulus *Es* (*Es*: Young's modulus). The yielding condition was judged based on von Mises criterion.

3.2.3 Sand cushion

Fig. 3(c) shows the constitutive law for sand cushion. To rationally analyze stress behavior of sand cushion when a heavy weight collides, second order parabolic stress-strain relation for sand cushion [5] was applied in which the constitutive relation is described in the following expression as shown in Fig. 3(c).

$$\sigma = 50\,\varepsilon^2 \tag{3.1}$$

Here, σ_{sand} is stress and ε_{sand} is the volumetric strain of sand element. Here, referring to the literature [5], material properties of sand for impact response analysis were assumed as: Young's modulus E_{sand} = 10 *GPa*; Poisson's ratio; ν_{sand} = 0.06; and density ρ_{sand} = 1,600 kg/m^3.

3.3 Equivalent fracture energy concept

Based on this equivalent fracture energy concept, each concrete element can retain the equivalent fracture energy due to setting a fictitious tensile strength corresponding to volume of element. In Fig. 5(a), assuming fracture energy of standard concrete element and volume of the element as G_f and V_0 respectively. G_f can be represented as Eqn. 3.2 in which f_{t0} and ε_{t0} are tensile strength and strain at tensile failure of the standard concrete element as shown in Fig. 5.

$$G_f = \frac{f_{t0}\varepsilon_{t0}}{2} V_0 \tag{3.2}$$

Ultimate tensile strain ε_{to} can be determined as the following equation described in Fig. 3(a)

$$\varepsilon_{t0} = \frac{f_{t0}}{E_c} \tag{3.3}$$

Assuming each element size in *x, y* and *z* direction of the standard element as x_o, y_o, and z_o, respectively, the volume of the standard element is as follows;

$$V_0 = x_0 y_0 z_0 \tag{3.4}$$

By putting the values of Eqns. 3.3 and 3.4, the fracture energy G_f can be obtained as,

$$G_f = \frac{f_{t0}^2}{2E_c} x_0 y_0 z_0 \tag{3.5}$$

Here, setting the fictitious tensile strength and element size in *y* direction of the *i*-element as f_{ti} and y_i and applying an equivalent fracture energy concept between standard element and *i*-element, following relationship can be obtained as;

$$\frac{f_{t0}^2}{2E_c} x_0 y_0 z_0 = \frac{f_{ti}^2}{2E_c} x_0 y_i z_0 \tag{3.6}$$

Fictitious tensile strength of *i*-element f_{ti} can be obtained as follows;

$$f_{ti} = f_{t0}\sqrt{\frac{y_0}{y_i}} \tag{3.7}$$

Therefore, taking the fictitious tensile strength f_{ti} obtained from Eqn. 3.7 for *i* element with y_i as the size in *y*-direction, the crack occurred in the *i*-element can be rationally estimated similar to f_{to} of the standard element with fracture energy G_f. The fictitious tensile strength for each element size in *y*-direction used in this study is listed in Table 3.3.

Table 3.3 Tensile strength for different analytical cases

Element size in span direction (mm)	Fictitious tensile strength (MPa)
250	1.18
83	2.04
50	2.64
35	3.12

4. COMPARISON OF RESULTS

4.1 Discussion of an applicability of equivalent tensile fracture energy concept

In order to investigate the practical applicability of proposed equivalent tensile fracture energy concept (hereinafter, G_f concept) for rationally analyzing impact response behavior of the prototype RC girder with sand cushion under falling-weight impact loading, numerical analysis results obtained using each mesh size listed in Table 3.3 with/without considering G_f concept were compared with the experimental results. Figure 6 shows the comparisons of impact force wave *P*, reaction force wave *R* at one supporting point, and deflection waves *D-1/2* shown in Fig. 1 for each case, in which *P*, *R*, and *Ds* are compared for 200 ms, 200 ms and 400 ms, respectively, from the beginning of impact.

Figure 6 shows the comparisons for the case of MS250. From Figs. 6(a) and 6(b) for the results of impact force wave *P* and reaction force wave *R*, following results were obtained: (1) influences of tensile fracture energy of concrete on impact force time history *P* may be not significant; (2) regarding reaction force time history *R*, considering without G_f concept, a half sine wave with smaller amplitude and long duration time at the beginning of impact occurs and duration time of the main wave is smaller to that of experimental results; and (3) on the other hand, in case considering with G_f concept, amplitude and duration time of the main wave are similar with those of experimental results. From the comparisons of deflection time histories *D-1/2* of Figs. 6(c) and 6(d), it is observed that in case considering without G_f concept, maximum amplitude of the waves are 50 % less than that of experimental results and vibration period in the free vibration state after unloading is almost half to that of the experimental ones. It suggests that the damage of the girder was underestimated. On the other hand, in case considering with G_f concept, it is confirmed that maximum amplitude and vibration period of the free vibration are in good agreement with the experimental results.

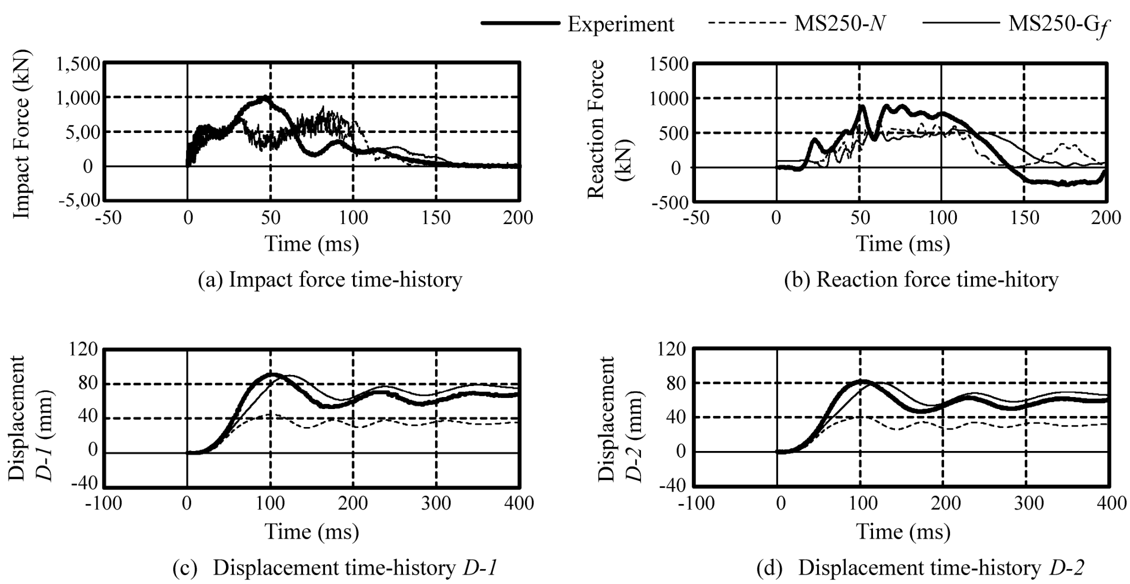

Figure 6 Comparison between experimental and analysis results with/without G_f

4.2 Comparison of numerical analysis results considering G_f

The applicability of the proposed method is examined for the set of each element length for different cases considering G_f in this section and comparing with experimental results. Analytical result concerning all cases with different element length considering G_f is compared with the experimental results as shown in Fig. 7. The comparison between results for coarse mesh with/without considering G_f are shown in Fig. 7.

The maximum value of impact force wave is smaller than the experimental results regardless of the mesh size of the element length as previously observed. It is understood that the response characteristics are similar regardless of the size of the element length as well as the case of impact force and for the reaction force waveform. From Fig. 7(b), it is confirmed that the reaction force wave at the one supporting point tends to be high amplitude in case of one-division was almost similar to experimental one. It is understood that the amplitude of *D-1/2* as shown in Figs 7(c) and 7(d), the both cycle and the residual displacement are in the state of a free vibration after the maximum displacement regardless of the size of the element length by comparing the experimental results and the analytical one. By comparing the experimental results, among four cases the most underestimating case is MS83-G_f though the level of the error margin is not large when seeing in detail. By converting the tensile strength as the case of MS35-G_f as shown in Table 3, and it can be confirmed to an analytical result of MS250-G_f when the element length is the largest then the analytical accuracy is good enough even if the element division is coarse. Even if the span direction element length is different from a standard element, it means that the mesh size up to seven times the standard element length having the same accuracy as the case to use a standard element by using the fracture energy concept.

5. CONCLUSIONS

This paper presents a detailed formulation and numerical implementation of an objectivity algorithm for equivalent fracture energy concept of prototype RC girder with sand cushion. In order to establish a modification method for material properties of concrete so as to rationally analyze using coarse mesh, an equivalent fracture energy concept for concrete element is proposed and the applicability was conducted comparing numerical analysis results and experimental results. From this study, it is confirmed that even though coarse mesh was used for RC girder with sand cushion, similar results with those obtained using fine mesh can be assured and are in good agreement with the experimental ones. The results obtained from this study are as follows;

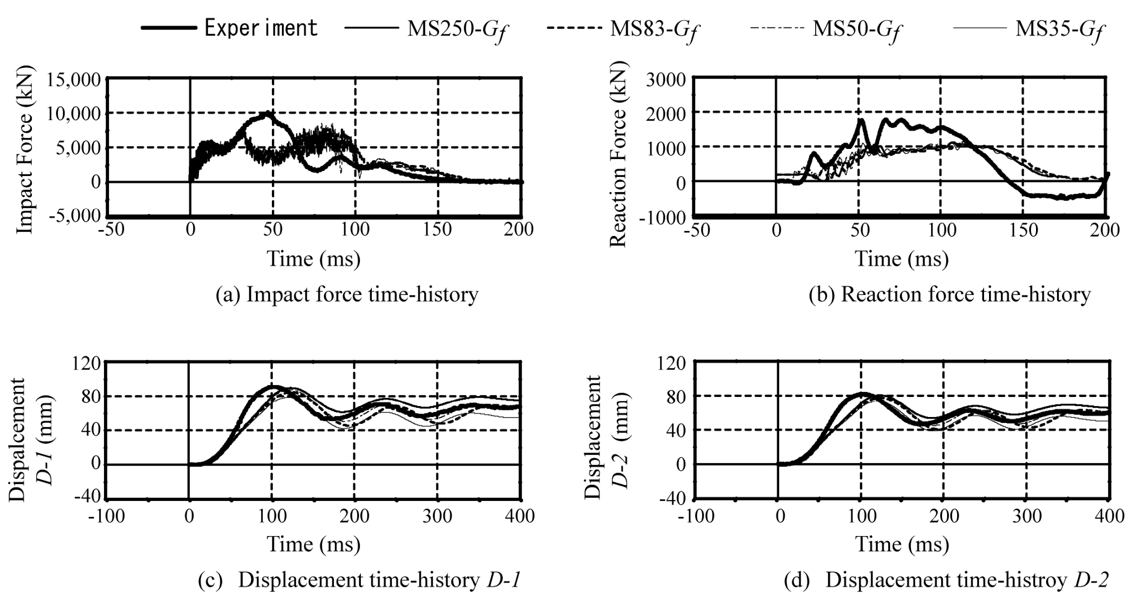

Figure 7 Comparison between experimental and analysis results considering G_f

(1) The fictitious tensile strength for coarse mesh has been proposed for the prototype RC girder with sand cushion
(2) By using the fictitious tensile strength for coarse mesh with 250 mm mesh size, similar degree of accuracy can be obtained by using the fine mesh having mesh size of 35 mm with sand cushion. However, an incident of the beginning of impact and maximum amplitude of the impact force time

(3) history tend to be underestimated by comparing with those of experimental results.

REFERENCES

[1] Kishi, N., Bhatti, A.Q., Okada, S., Konno, H.,: (2006). "An applicability of impact response analysis method for prototype RC girders under falling-weight impact loading" Journal of Structural Engineering, JSCE, 52A, 1261-1272.
[2] Hallquist, J.O., (2000). "LS-DYNA User's Manual." Livermore Software Technology Corporation.
[3] Japan Society of Civil Engineers (2002). "Standard Specifications for Concrete Structures-2002 "Structural Performance Verification" JSCE, (in English).
[4] Bhatti, A.Q., Kishi, N., Konno, H. and Okada, S.: (2006). "Effective finite element mesh size distribution for proposed numerical method of prototype RC girders under falling-weight impact loading", Proceedings of 2nd International Conference on Design and Analysis of Protective Structures, *DAPS* Singapore, November 13-15, 261-272.
[5] Bhatti, A.Q., Kishi, N., Konno, H. and Okada, S.: (2006) "An Impact Response Analysis of Large Scale RC Girder With Sand Cushion" Proceedings of JCI, Niigata, July 07, Vol. 28 No.2, 871-876.